Position Estimation of an Underground Acoustic Source by a Passive Sonar System

Soon Suck Jarng
Dept. of Control & Instrumentation Eng., Chosun University, ssjarng@mail.chosun.ac.kr

Abstract

The aim of the work described in this paper is to develop a complex underground acoustic system which detects and locates the origin of an underground hammering sound using an array of six hydrophones located about 100m underground. Two different methods for the sound localization will be presented, a time-delay method and a power-attenuation method. In the time-delay method, the cross correlation of the signals received from the array of sensors is used to calculate the time delays between those signals. In the power-attenuation method, the powers of the received signals provide a measure of the distances of the source from the sensors.

ACKNOWLEDGMENTS

This study was granted by STEPI (Science & Technology Policy Institute) Korea, as 1998 international program of co-work of research between Korea and United Kingdom.

1. INTRODUCTION

The ability to detect and determine the position of an underground sound source is desirable both for civilian and military purposes, for example, for rescue following collapse of mining tunnels, or for the detection of covert underground operations.[1,2,3] Compared to the similar problem in air or in water there are a number of features which cause additional difficulties - the medium is likely to be inhomogeneous with unknown properties, objects which scatter sound are usually present, and there are practical difficulties in positioning (and moving) the acoustic sensors. A suitable acoustic system might consist of a number of acoustic sensors positioned in the suspected locality of the sound source (Fig. 1). Fig. 2 shows an overall layout of underground experimental apparatus.

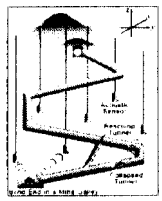

Fig. 1 An underground passive SONAR system could be commercially applicable for safety rescue following collapse of mining tunnels.

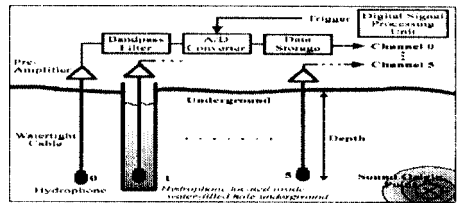

Fig. 2 The overall layout of the underground experimental apparatus

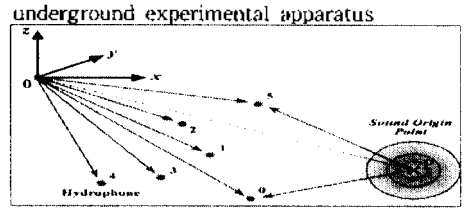

Fig. 3 The position of the underground sound origin could be evaluated from time delays and geographical coordinates.

The aim of this paper is to develope a complex underground acoustic system which detects and localizes the origin of an underground hammering sound using an array of hydrophones positioned about 100m underground. Three numerical estimating algorithms of the sound localization will be presented.

2. METHODS

6 underground holes were bored vertically to the ground. Their diameters are 15cm and the depth of each hole is about between 80m and 120m. After vertical drilling, the underground tunnels were naturally filled with water. A hydrophone was set at or near the bottom of each of the underground water-filled tunnels. Bruel & Kjaer type 8106 hydrophones (Table 1) were used with a 150m watertight low-impedance core cable (B&K AC0101) for the work.

Two different numerical methods were developed for underground acoustic sound localization. The first method is a time-delay method and the second method is a power-attenuation method. The time-delay method uses relative time delay information between different input signals and the power-attenuation method uses relative power information between input signals. Since those methods carry out numerical solutions, more number of signal channels would improve estimating power in greater. In this work, six hydrophones were used.

2.1 TIME-DELAY METHOD

Consider six hydrophones randomly located underground (Fig. 3). Their global coordinates are $[x_i, y_i, z_i]$ for $(0 \le i \le 5)$. Any global position of the sound origin is assumed to be $[x_p, y_p, z_p]$. ΔT_{0i} is defined as a time delay between the first hydrophone and the i^{th} hydrophone and V is the unknown velocity of the acoustic propagation. The first hydrophone is taken as a reference sensor while other hydrophones are considered as objective sensors. In the time-delay method, a sound origin is estimated by minimizing a cost function which relates distance differences between the 0^{th} sensor position and other sensor positions with time delays multiplied by the unknown sound propagation velocity;

$$F(x,y,z,V) = \sum_{i=1}^{5} (r_i - r_0 - \Delta T_{0i} \cdot V)^2 \quad (1)$$

where $r_0 = \sqrt{(x_0-x)^2+(y_0-y)^2+(z_0-z)^2}$,

$r_i = \sqrt{(x_i-x)^2+(y_i-y)^2+(z_i-z)^2}$ and [x, y, z] is an arbitrary coordinate. Different x, y, z, and V are applied to the cost function in order to find optimal values of x, y, z, and V which are an estimated sound origin and a propagation velocity.

Time delays between hydrophones are calculated by correlating one channel signal to the other[4];

$$\gamma_{xy}(m) = \frac{1}{N-|m|} \sum_{k=1}^{N-|m|} x(k)y^*(k+m) \quad (2)$$

where N is the total number of discrete signals. It is an unbiased form of cross-correlation estimation. Since an input acoustic signal is mixed with various unwanted noise, the result of the correlation is often incorrect. It is always better to have higher sampling frequency in data acquisition.

2.2 POWER-ATTENUATION METHOD

A hammering shock generated from an underground tunnel is propagated to hydrophones through rocks and soils. From discrete pressure data, P(k), measured by the i^{th} hydrophone, acoustic power, I_i, is calculated;

$$I_i = \frac{1}{N} \sum_{k=0}^{N-1} P^2_{S+N}(k) - \frac{1}{N} \sum_{k=0}^{N-1} P^2_N(k) \quad (3)$$

where subscripts S and N represent signal and noise. The attenuation of the acoustic power as underground elastic waves are propagated through underground media depends on distance and material properties. It might be modelled as follows[5];

$$I(r) = I_0 \cdot (\frac{1}{r})^2 \cdot 10^{\alpha(r-1)} \quad (4)$$

where α is material attenuation coefficient [dB/M] and I_0 is an initial power of the hammering shock.

In the power-attenuation method, a sound origin is estimated by minimizing a cost function which relates measured power ratios between the 1^{st} sensor and other sensors with modelled power ratios;

$$F(x,y,z,\alpha) = \sum_{i=1}^{5} [\Delta P_{0i} - (\frac{r_i}{r_0})^2 \cdot 10^{\alpha(r_i - r_0)}]^2 \quad (5)$$

where ΔP_{0i} $(= I(r_0)/I(r_i))$ is defined as a power ratio between the first hydrophone and the i^{th} hydrophone.

The algorithm of the Nelder-Meade simplex search method is used for estimating (x, y, z), α and V[6,7] from 6 measured acoustic powers.

3. RESULTS AND DISCUSSION

Table 2 shows cartesian co-ordinates of 6 hydrophones located at the bottom of the water-filled tunnel. Z-axis is based on sea surface as 0m. There might be practically expected some spatial deviation in sensor position because any vertical drilling underground could be twisted. The exact sensor position is not known. Fig.4 schematically shows 6 hydrophones' locations and a hammering position

Table 2. 6 hydrophone locations and a hammering position

Sensor No.	X axis [m]	Y axis [m]	Z axis [m]	Distance from Hammering Position [m]
0	593.5	671.4	338.7	99.8
1	608.7	656.4	366.8	98.4
2	688.3	600.2	376.3	122.1
3	673.6	594.2	354.9	124.0
4	701.0	644.8	341.7	74.9
5	668.1	640.3	371.7	84.3
Hammering Position	682.0	717.3	342.3	0

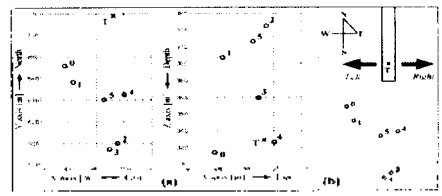

Fig. 4 hydrophone locations (o) and a hammering position (x)

Fig. 5 shows typical time responses of hammering stimuli on the underground tunnel. And Fig. 6 shows the FFT spectra of the corresponding time responses. It is meaningful to notice that even though the spectrum of each time response is calculated for the same hammering event, the pattern of the spectrum is significantly different from each other. This is interpreted as that the elastic wave of the hammering shock is changed in its spectrum while it is propagated through soils and rocks. Because of this phenomena, it is always difficult to calculate correct time delays between received signals by cross correlation technique[8].

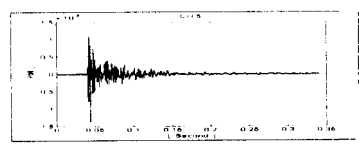

Fig. 5 Time Responses of Underground Hammering Shocks

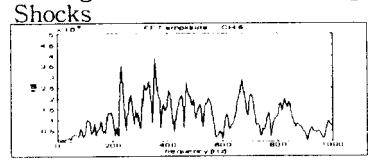

Fig. 6 FFT Spectra of Underground Hammering Shocks

3.1 TIME-DELAY METHOD RESULTS

A time delay can be theoretically calculated if the difference, between one distance which is between a reference sensor position and the sound origin and the other distance for the other objective sensor position, and the sound propagation velocity are known. Table 3 shows theoretical time delays between different reference sensors and objective sensors. The sound propagation velocity is assumed to be between 5000m/sec and 7000m/sec. Measured time delays are assumed to be in those range, but real data are occasionally quite different from theoretical values.

Table 4 shows measured time delays between different reference sensors and objective sensors. Time delay values are not diagonally symmetrical because of noise in the signal. There are quite significant differences between Table 3 and Table 4.

Table 2 Theoretical time delays between different reference sensors and objective sensors. (V : 5000m/sec ~ 7000m/sec) [10^{-3} sec]

Obj / Ref	0	1	2	3	4	5
0	0.0	-0.2 ~ -0.3	3.2 ~ 4.5	3.5 ~ 4.9	3.5 ~ 5.0	-2.2 ~ -3.1
1	0.2 ~ 0.3	0.0	3.4 ~ 4.7	3.7 ~ 5.1	-3.3 ~ -4.7	-2.0 ~ -2.8
2	-3.2 ~ -4.5	-3.4 ~ -4.7	0.0	0.3 ~ 0.4	-6.7 ~ -9.4	-5.4 ~ -7.6
3	-3.5 ~ -4.9	-3.7 ~ -5.1	-0.3 ~ -0.4	0.0	-7.0 ~ -9.8	-5.7 ~ -7.9
4	3.5 ~ 5.0	3.3 ~ 4.7	6.7 ~ 9.4	7.0 ~ 9.8	0.0	1.3 ~ 1.9
5	2.2 ~ 3.1	2.0 ~ 2.8	5.4 ~ 7.6	5.7 ~ 7.9	-1.3 ~ -1.9	0.0

Table 5 shows the estimated location of the sound origin and the estimated sound propagation velocity by the time-delay method. The estimated location with the 1st reference sensor is much closer to the true origin than those with the 6th reference sensor.

Table 3 Measured time delays between different reference sensors and objective sensors. [10^{-3} sec]

Ref \ Obj	0	1	2	3	4	5
0	0.0	0.2	4.3	4.4	-3.4	-1.2
1	-0.3	0.0	4.0	4.1	-4.2	-1.4
2	-4.3	-4.0	0.0	0.2	-8.1	-5.3
3	-4.4	-4.1	-0.1	0.0	-8.3	-5.5
4	3.4	4.3	8.0	8.2	0.0	2.8
5	1.2	1.4	5.2	5.5	-2.8	0.0

Table 4 The difference between the true origin and the estimated location by the time-delay method

Reference Channel No	Difference between the true origin and the estimated location [m]				Estimated Velocity [m/sec]
	dX	dY	dZ	$\sqrt{dZ^2+dY^2+dZ}$	
0	1.996	10.000	-10.050	14.3174	6500
1	5.996	18.000	-13.050	23.0273	6330
2	12.000	29.000	-16.050	35.2506	6439
3	7.996	19.000	-17.050	26.7514	6390
4	6.996	20.000	-22.050	30.5802	6359
5	21.000	44.000	-18.050	51.9885	6637

One of comparative methods to find any reason of the difference between the true origin and the estimated location of Table 5 is normalizing distance differences (Table 6) as well as normalizing measured time delays (Table 7). In Table 6 distance differences between the distance between the reference sensor and the sound origin and the distances between objective sensors and the sound origin are normalized. And In Table 7 measured time delays are normalized with each of reference sensors. And Table 8 shows the difference between Table 6 and Table 7.

Table 5 Normalized distance differences with each of reference sensors

Ref \ Obj	0	1	2	3	4	5
0	0.0000	-0.0555	0.8994	0.9775	-1.0000	0.6221
1	0.0537	0.0000	0.9244	1.0000	-0.9143	-0.5485
2	-0.4753	-0.5027	0.0000	0.0411	-1.0000	-0.8011
3	-0.4943	-0.5224	-0.0395	0.0000	-1.0000	-0.8089
4	0.5057	0.4776	0.9605	1.0000	0.0000	0.1911
5	0.3889	0.3542	0.9512	1.0000	-0.2362	0.0000

The absolute sum of each column indicates how much the corresponding sensor falsely influences to other sensors in the calculation of the time delay. In Table 8 the 6th sensor has the highest value, 1.008, than other sensors. That is why the difference between the true origin and the estimated location with the 6th reference sensor is bigger than others in Table 5. Fig. 7 and Fig. 8 show differences between normalized theoretical distance differences (O) and normalized measured time delays (X) with the 1st reference sensor and the 6th reference sensor respectively.

Table 6 Normalized time delays with each of reference sensors

Ref \ Obj	0	1	2	3	4	5
0	0.0000	0.0455	0.9773	1.0000	-0.7727	-0.2727
1	-0.0714	0.0000	0.9524	0.9762	-1.0000	-0.3333
2	-0.5309	-0.4938	0.0000	0.0247	-1.0000	-0.6543
3	-0.5301	-0.4940	-0.0120	0.0000	-1.0000	-0.6627
4	0.4146	0.5244	0.9756	1.0000	0.0000	0.3415
5	0.2182	0.2545	0.9455	1.0000	-0.5091	0.0000

Table 7 Differences between normalized distance differences and normalized time delays

Ref \ Obj	0	1	2	3	4	5
0	0.0000	0.1010	0.0779	0.0225	0.2273	0.3494
1	-0.1251	0.0000	0.0280	-0.0238	-0.0857	0.2152
2	-0.0556	0.0089	0.0000	-0.0164	0.0000	0.1468
3	-0.0358	0.0284	0.0275	0.0000	0.0000	0.1462
4	-0.0911	0.0468	0.0151	0.0000	0.0000	0.1504
5	-0.1707	-0.0997	-0.0057	0.0000	-0.2729	0.0000
$\sum \lvert x \rvert$	0.4783	0.2848	0.1542	0.0627	0.5859	1.0080

Fig. 7 Differences between normalized theoretical distance differences (O) and normalized measured time delays (X) with the 1st reference sensor

Fig. 8 Differences between normalized theoretical distance differences (O) and normalized measured time delays (X) with the 6th reference sensor

3.2 POWER-ATTENUATION METHOD RESULTS

Table 9 shows measured power ratios between different reference signal channels and objective signal channels. And Table 10 shows the estimated location of the sound origin and the estimated attenuation coefficient by the power-attenuation method. The estimated location with the 6th reference sensor is much closer to the true origin than those with the 2nd reference sensor. Fig. 9 shows the measured acoustic power (X) and numerically estimated power (O) of the hammering shock against distance. The continuous line indicates the trend of the acoustic power attenuation against distance with α=0.0164 which is an optimized attenuation coefficient. The upper and the lower dashed lines are the bounds of the power attenuation. The attenuation coefficients for the upper and lower bounds are 0.0205 and 0.0131 respectively.

Table 8 Measured power ratios between different reference signal channels and objective signal channels

Ref \ Obj	0	1	2	3	4	5
0	1.0000	0.3745	0.5637	0.3320	4.1197	2.6409
1	2.6701	1.0000	1.5052	0.8866	11.0000	7.0515
2	1.7740	0.6644	1.0000	0.5890	7.3062	4.6849
3	3.0116	1.1279	1.6977	1.0000	12.4070	7.9535
4	0.2427	0.0909	0.1368	0.0806	1.0000	0.6410
5	0.3787	0.1418	0.2135	0.1257	1.5599	1.0000

Table 9 The difference between the true origin and the estimated location by the power-attenuation method

Reference Channel No	Difference between the true origin and the estimated location [m] dX	dY	dZ	$\sqrt{dZ^2+dY^2+d}$	Estimated Attenuation
0	-9.891	-20.56	-7.631	24.0578	0.02120
1	-19.00	-64.00	-15.050	68.4361	0.03192
2	9.996	-14.00	12.950	21.5319	0.01404
3	0.996	-18.00	5.952	18.9847	0.01736
4	-11.00	-41.00	7.048	43.0311	0.01712
5	8.532	-5.901	14.40	17.7476	0.01801

Fig. 9 Measured acoustic power (X) and numerically estimated power (O) of the hammering shock against distance. The continuous line indicates the trend of the acoustic power attenuation against distance.

The localization error of Table 10 is mainly caused by environmental noise in measurements. With the optimized attenuation coefficient, α=0.0164, power ratios between different reference signal channels and objective signal channels can be theoretically calculated using Equ. (4) as in Table 11. And Table 12 shows differences between theoretical power ratios and measured power ratios for different reference sensors respectively. The most significant difference happens for the 2nd reference sensor such as 1295.5%.

4. CONCLUSION

In the present underground localization, the sound propagation velocity and the power attenuation coefficient of the underground media are assumed to be constant for every channels for simplicity. Both the time-delay method and the power-attenuation method produce quite reasonable results of underground sound localization. After several detections and localizations for the similar hammering events, the statistically averaged estimated origin of the hammering shock might be closer to the true origin. With such estimation of less than 30m difference, the true origin of the hammering location could be discovered by a geophone at the suspected area[2,3].

Table 10 Theoretical power ratios with α=0.0164 between different reference signal channels and objective signal channels

Ref \ Obj	0	1	2	3	4	5
0	1.0000	1.0830	0.2878	0.2593	4.5161	2.5051
1	0.9234	1.0000	0.2658	0.2394	4.1700	2.3131
2	3.4741	3.7624	1.0000	0.9007	15.6893	8.7028
3	3.8571	4.1772	1.1102	1.0000	17.4189	9.6622
4	0.2214	0.2398	0.0637	0.0574	1.0000	0.5547
5	0.3992	0.4323	0.1149	0.1035	1.8028	1.0000

Table 11 Difference between theoretical power ratios and measured power ratios for different reference sensors respectively [%]

Ref \ Obj	0	1	2	3	4	5	$\sum \lvert x$
0	0.0000	65.3979	96.3732	28.2906	8.7614	5.3891	204.2
1	188.99	0.0000	467.517	270.759	163.679	204.574	1295.5
2	49.076	82.3794	0.0000	34.6700	53.5382	46.332	266.0
3	22.052	73.0283	53.0690	0.0000	28.8813	17.851	194.9
4	9.6027	62.0751	115.230	40.6100	0.0000	15.509	243.0
5	5.1135	67.1672	86.3316	21.7305	13.427	0.0000	193.8

5. REFERENCES

[1] Ballard R.F., "Tunnel Detection" U.S. Army Engineer Waterways Experiment Station, Technical Report GL-82-9, 1982.

[2] Greenfield R.J., "Seismic Analysis of Tunnel Boring Machines Signals at Kerckhoff Tunnel", U.S. Army Engineer Waterways Experiment Station, Miscellaneous Paper GL-83-19, 1983.

[3] Greenfield R.J., "The WES Seismic Listening System (SLS)", reported by U.S. Army Engineer Waterways Experiment Station, Vicksburg, Mississippi, 1987.

[4] J.S. Bendat and A.G. Piersol, "Random Data: Analysis and Measurement Procedures", p. 332, John Wiley and Sons, 1971.

[5] Ben-menahem A. and Singh S.J. "Seismic Waves and Sources", published by Springer-Verlag, pp. 1056, 1981.

[6] Nelder J.A. and Mead R., "A simplex method for function minimization", Computer Journal, Vol. 7, PP:308-313. 1965.

[7] Dennis J.E., Jr. and Woods D.J., "New computing environments microcomputers in large-scale computing", edited by A.Wouk, SIAM, PP:116-122, 1987.

[8] A.V. Oppenheim and R.W. Schafer, "Digital Signal Processing", Prentice-Hall, pp.539, 1975.